Geomechanics and Engineering, *Vol. 32, No. 6 (2023) 567-581*
https://doi.org/10.12989/gae.2023.32.6.567

Influence of dual layer confinement on lateral load capacity of stone columns: An experimental investigation

Akash Jaiswal* and Rakesh Kumar[a]

Department of Civil Engineering MANIT, Bhopal,462003, India

(*Received August 19, 2022, Revised February 5, 2023, Accepted February 15, 2023*)

Abstract. Enhanced vertical load capacity of the ground reinforced with the stone columns drew great attention by the researchers as it deals with many of the geotechnical difficulties associated with the weak ground. Recently, it has been found that the stone columns are also prone to fail under the shear load when employed beneath the embankments or the foundations susceptible to lateral loads. In this study, the effect of various encasement conditions on the lateral deflection of stone columns is investigated. A method of dual layers of encasement has been introduced and its the effect on lateral load capacity of the stone columns has been compared with those of the single encased stone column and the un-encased stone columns. Large shear box tests were utilised to generate the shear deformation on the soil system under various normal pressure conditions. The stiffness of the soil-stone column combined system has been compared for various cases of encasement conditions with different diameters. When subjected to lateral deformation, the encased columns outperformed the un-encased stone columns installed in loose sand. Shear stress resistance is up to 1.7 times greater in dual-layered, encased columns than in unencased columns. Similarly, the secant modulus increases as the condition changes from an unencased stone column to single-layer encasement and then to dual-layer encasement, indicating an improvement in the overall soil-stone column system.

Keywords: dual layer; encasement; lateral load; shear modulus of elasticity; stone column

1. Introduction

Weak soil deposits cause high settlement in embankments, due to possible bearing failure, excessive settlement, building structures on such soil is difficult for geotechnical engineers. Many ground improvement techniques have been studied and utilised by the engineers, such as using admixtures include cohesive non-swelling soils (Murty and Praveen 2008), fly ash (Phanikumar and Sharma 2004), lime (Shirohammadi *et al.* 2021), lime-zeolite (Khajeh 2022), cement stabilisation (Kowalski *et al*. 2007) and geopolymers (Khaksar Najafi *et al.* 2021a, b) for modification of the mechanical or engineering properties of the soil. Numerous unconventional soil stabilisers have also been used (Khajeh 2020). The use of soil-Expanded Polystyrene in the form of beads and blocks has been researched and proposed in a variety of combinations (Khajeh *et al.* 2020, Khajeh *et al.* 2021). Similarly, electro-osmosis (Martin, L. *et al.* 2019), geosynthetic reinforcement (Dash *et al.* 2004, Guo *et al.* 2020) and stone column/granular pile (Abhishek *et al.* 2016) are extremely well known to engineers when confronting weak or unstable soil.

For strengthening weak soil under the embankments, compacted granular columns are one of the most prevalent and convenient approaches because of their significant improvement in load bearing capacity by the soil arching phenomenon (Terzaghi 1944, Hewlett 1988, Low *et al.* 1994, Deb and Mohapatra 2013, Han and Gabr 2002, Yun-min *et al.* 2008, Han and Ye 2001), acceleration in consolidation, post-construction settlement, short-term stability, and liquefaction mitigation (Mitchell and Huber 1985, Priebe 1995, Poorooshasb and Meyerhof 1996, Gniel and Bouazza 2009, Deb and Dhar 2011, Ali *et al*. 2014, Buddhima *et al.* 2013, Ng and Tan 2014, Hosseinpour *et al.* 2016, Das and Deb 2017, Bhattacharya and Kumar 2017, Elsawy 2013, Ghazavi and Afshar 2013, Dash and Bora 2013, Lima *et al.* 2019, Sadr and Hataf 2021, Gao *et al.* 2021).

In very weak soil, the intervening soil is unable to support and resist the bulging of the stone column and soft clay penetrates into aggregate voids (McKenna *et al*. 1975), the behaviour of stone column can be improved by the lateral confinement (Van Impe 1989, Katti *et al.* 1993). In the recent decade of the twenty first century the research related to use of encasement as wrapping material to the stone column has been extensively studied by conducting the laboratory model test (Murugesan and Rajagopal 2006, Yoo and Lee 2012, Black *et al.* 2007a , Malarvizhi and Ilamparuthi 2007, Gneil and Bouazza 2009, Murugesan and Rajagopal 2010, Wu and Hong 2014) followed by the theoretical or numerical analysis (Raithel and Kempfert 2000, Raithel *et al*. 2005, Murugesan and Rajagopal 2007, Almeida *et al.* 2013, Chen 2009, Castro *et al.* 2013, Yoo 2010, Castro and Sagaseta 2011).

Geosynthetic (including geotextile, geogrid, and geonet) encased stone columns have been utilised to address the inadequacies without lateral confinement. This encasement

*Corresponding author, Ph.D. Scholar
E-mail: akashcivilengg777@gmail.com
[a]Associate Professor

http://www.techno-press.org/?journal=gae&subpage=7
ISSN: 2005-307X (Print), 2092-6219 (Online)

increases the overall stiffness as a higher vertical load will be transferred to the surrounding soil by the bulging phenomenon. (Alkhorshid *et al.* 2019, Murugesan and Rajagopal 2010, Pulko *et al.* 2011, Kong *et al.* 2018, Gniel and Bouazza 2010, Gholaminejad *et al.* 2020, Xu *et al.* 2021, Xue *et al.* 2019, Basack *et al.* 2017, Gu *et al.* 2020, Ou-Yang *et al.* 2017, Almeida *et al.* 2015, Chen *et al.* 2015, Li *et al.* 2020, Zhang *et al.* 2012, Elsawy 2013, Alexiew *et al.* 2005, Brokemper *et al.* 2006, Maheshwari and Chauhan 2013, McCabe *et al.* 2013, Shahu and Reddy 2014, Ali *et al.* 2014, Zhou and kong, 2019a, b).

In an effort to increase the vertical load-bearing capacity of the column, attention was focused on the bulging failure of the column; however, failures due to the deep-seated failure of the column group were identified. External and internal stabilities are highlighted by Kitazume and Maruyama (2006, 2007) in the design technique as important failure patterns, they state the Probability of combined stone column and surrounding soil slide failure in external stability without column rearrangement. In addition, the numerical study conducted by Han *et al.* (2005) Under the embankments, this rotational failure for the deep mixed column may be the dominant one. The plane of the slip circle traversing the stone column functions as the shear failure plane for the column body, which is the most common mode of failure for compacted sand or gravel (Abusharar and Han 2011). Bending moment and shear force diagrams from the study of Chen *et al.* 2015, demonstrated that failure initiates in the columns at the edge of the slope because of the lower amount of lateral resistance. Granular columns under the embankment edge have an increased risk of failure, as Khabbazian *et al.* (2015) found through numerical analysis. Many of the researchers studied and analysed the behaviour of stone columns under lateral load.

Mohapatra *et al.* (2016) investigated the shear behaviour of conventional and geosynthetic-encased granular columns under lateral strain in a sand bed created in a large shear box setup. When the geosynthetic-encased granular column was compared to a conventional granular column, the shear resistance of the geosynthetic-encased granular column was found to be significantly greater. Geosynthetic encasement improves granular column lateral load capability by mobilising tensile forces. Two types of failure have been defined: OGC failure in shear along the shear plane and bending type deformation in the case of an encased stone column influenced by the flexibility of geosynthetic encasement.

Naeini and Gholampoor (2019), investigated the shear strength of the clay bed reinforced by ordinary and encased stone columns under various conditions of stone column and encasement. The results reveal that the overall friction angle of the clay and stone column system increases, although there is little effect on the apparent cohesiveness. As the amount of clay that is being replaced or the normal pressure is raised, the shear capacity increases.

Nazariafshar and Aslani (2020) conducted an experimental study on different arrangements of stone columns installed in the clay bed. They concluded that a group of stone columns mobilises higher strength than a single column. The installation pattern does not affect the shear capacity of the stone column much if the area replacement is kept constant, whereas with the change of area replacement, the square pattern of arrangement shows the highest resistance to lateral load. They also compared the results of the experiments to the results of the analysis and found that the analytical results were more conservative.

Aghili *et al.* (2021) studied the influence of granular columns on treated clay with respect to cyclic shear characteristics. Various properties of clay, columns granular column and cyclic load parameters were modified to analyse treated clay behaviour. Experiments indicated that granular columns enhanced maximum cyclic shear resistance by 30% relative to untreated clay, especially in the beginning loading cycles. Increasing loading cycles reduces the damping ratio, increasing column diameter and aggregate density reduce the value. With more loading cycles, shear stiffness decreased.

Cengiz *et al.* (2019) studied unit cells, including OSCs and GECs, under static and cyclic lateral stresses, A unit cell shear device was utilized to simulate the unit cells near the toe of an embankment, where the column is liable to fail under shear. Under static and cyclic lateral stress, the failure envelope and strength characteristics of a granular-encased column with different reinforcing stiffnesses are quantified. Under static shear, the internal friction of the column-unicell composite was observed to increase as the stiffness of the reinforcement provided in the granular- encased column increased.

It is evident from the literature that the shear failure of the stone column is just as essential as the bulging when analysing and designing the failure of the body. Numerous studies have been conducted to examine and comprehend the behaviour of stone columns under lateral loads, which requires further development. As the stiffness of the encasement impacts the shear capacity of the column (Cengiz *et al.* 2019) and the column does not rupture completely when it is encased (Mohapatra *et al*. 2016), this provides the direction for the new concept that the two layers of the encasement could be used in the column body. In the present study, an attempt was made to comprehend the behaviour of stone columns installed in loose sand in dry state under lateral load for various encasement circumstances, namely dual layer encasement (DLE) and single-layer encasement (SLE). The alteration of the diameter of the stone column and the normal pressures have been investigated experimentally for three configurations of the stone column body, namely the single column test, group column tests, and the triangular and square arrangements. The stress-strain response of the combined system has been analysed using the shear modulus of elasticity.

2. Laboratory model

2.1 Material used

The sand bed was created in the same way that the

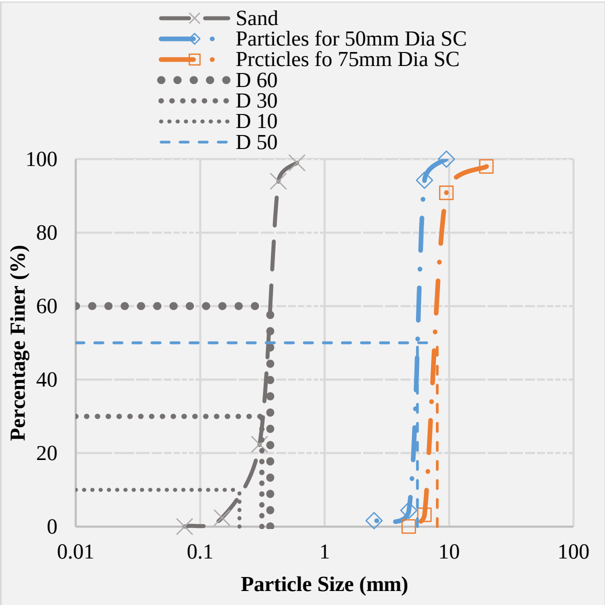

Fig. 1 Particle size distribution for sand and aggregate samples

Table 1 Properties of Sand and Aggregate

Parameters	Sand	Aggregate-1	Aggregate-2
Working Density (kN/m^2)	15.1	17.9	17.7
C_c	1.30	0.973	0.966
C_u	1.77	1.18	1.27
D_{10}	0.21	4.90	6.60
D_{30}	0.31	5.20	7.31
D_{50} (Avg. Size of Particle)	0.35	5.57	8.04
D_{60}	0.37	5.75	8.40
Cohesion (kN/m^2)	4	1	1
Friction Angle (°)	27	46	48

minimum density on the relative density test apparatus was obtained using the pouring device. The amount of dry sand to be used for the fixed volume in the test setup for a height of 150 mm was calculated prior to the filling process, and efforts have been made to use the exact amount for the required height of the sample. The obtained minimum density of the sand was 15.1 kN/m^2 for the sand bed. Fig. 1 represents the gradation curve for the sand and represents the characteristics used for the classification. Various aggregate class were used for creation of different size of the stone column to maintain the column to aggregate ratio near to 6-7 as suggested by (Fox 2011, Stoeber 2012). The average size (D_{50}) of the aggregate particles used in the stone column of size 50 mm was 5.2 mm, named Aggregate-1, whereas in the case of the 75 mm diameter stone column, this was maintained at 7.9 mm, named Aggregate-2. The maximum particle size recommendations made by Nayak (1983), according to which the size of the particle utilized within the stone column body should be smaller than 1/5 of the diameter of the stone column, are

(a)

(b)

Fig. 2 Aggregate samples prepared for infill material of (a) 50 mm and (b) 75 mm diameter

also satisfied. Various properties of the aggregates are indicated in the Table 1. The prepared sample of stone column infill is shown in the Fig. 2 for various stone column diameters. In the case of encased stone column, material of the column was wrapped by the use of Geonets, the secant modulus of the geonets used were 150 kN/m.

2.2 Large scale shear device

The large direct shear box setup, consisting of the upper and lower units, was used for the experimental program. The lower unit travels horizontally on rollers, and the upper unit is entirely resistant to lateral motion. The plan area of the box was 93,025 mm^2, and after accommodating the adjustment of the loading plate and grid, the actual sample height within the shear box was maintained at 150 mm. The normal load is applied by resting the loading frame on a load pad, and the lever arm is adjusted by using balancing equipment as the spirit level. The maximum permitted shear displacement in the available configuration was 50 mm, and the shear displacement was measured using an LVDT attached to the bottom box. The soil samples were sheared at a constant strain rate of 1 mm/min. The horizontal and vertical displacements with shear stress are displayed on the touch screen and display.

2.3 Sample preparation

In the experimental programme, three types of samples were prepared: an un-encased stone column, a single-

Table 2 Variations Considered for experimental study

Diameter (mm)	Arrangement	Type of Encasement	Nomenclature
50	Single Column	USC	50 S U
		SLE	50 S SL
	(Grouped) Triangular	USC	50 GT U
		SLE	50 GT SL
	(Grouped) Square	USC	50 GS U
		SLE	50 GS SL
75	Single Column	USC	75 S U
		SLE	75 S SL
		DLE	75 S DL
	(Grouped) Triangular	USC	75 GT U
		SLE	75 GT SL
		DLE	75 GT DL
	(Grouped) Square	USC	75 GS U
		SLE	75 GS SL
		DLE	75 GS DL
Sand Bed			
(Each Case is considered for 3 different Normal Pressures)			

layered encased (SLE) stone column, and a dual-layered encased (DLE) stone column. For testing the un-encased stone column, open-ended steel tubes with inner diameters equal to 50 and 75 mm were kept in the desired location at the base of the lower half of the large shear box set up to build the triangle or square arrangement of the stone column as well as the single stone column. For each experiment, a known amount of dry sand was put in the shear box around the steel tubes, the entire box was filled till the require height of 150 mm without compaction, resulting in the lowest density sand bed that provided the relative density of 41%. A sieved sample of the aggregate required based on the stone column diameter to particle size ratio was taken for a specific column size, and the measured quantity was compacted in three equal layers inside the steel tubes. A steel tamping rod with an 8-mm diameter was dropped from a fixed height to densify the aggregates in five layers. Tampering falls from a predetermined height were used to tamper with each layer. The same process was used in different setups to check out the relative density of the created stone column, which came out to be 69% for Aggregate-1 and 67% for Aggregate-2. After the aggregate was poured and packed to the full height of the shear box, the steel tubes were slowly pulled up and away from the sand bed. By utilising steel tubes with smooth interior and exterior surfaces, the granular column and surrounding sand disturbance were reduced.

Encased stone columns were also erected in a similar manner with the geonet pasted temporarily on the steel tube, after completing the material filling procedure, the steel tube was taken out of the bed, leaving the geonet layer in place. In case of dual-layered stone column two steel tubes were used instead of one, with the geonet layer positioned at the inner location of the column body so that both layers could be generated, as shown in Fig. 3(a).

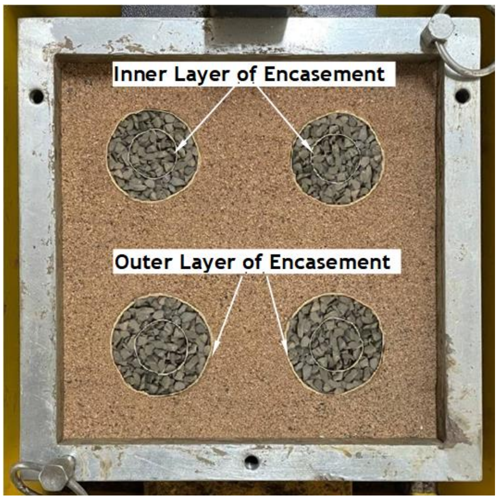

(a) 75GS DL

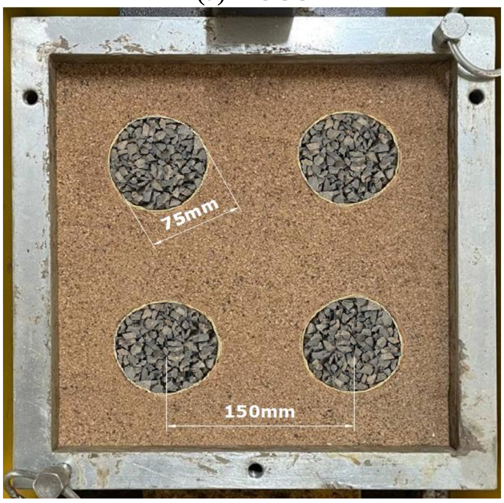

(b) 75 GS SL

(c) 50 GT SL

Fig. 3 Installed Stone columns for experimental Study

The 50 mm and 75 mm diameter single columns and gro uped columns (triangular and square arrengements) were tested for cases of un-encased columns and single-layer. Double layered stone column was not feasible to create in the small diameter of the 50 mm, only tested for the 75 mm

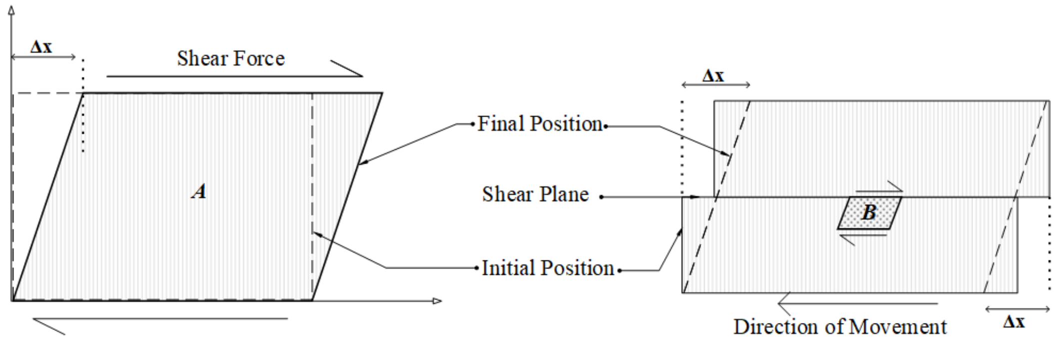

Fig. 4 Consideration of soil element under the shear load

diameter stone columns. The spacing between the stone column in the study is twice the of stone column diameter for all the cases where group of stone column is installed. Figs. 3(b) and 3(c) illustrates a single-layered stone column with a square pattern for columns with a 75 mm diameter and a triangular pattern for columns with a 50 mm diameter. The lateral deformation of 25% has been generated under various normal pressures of 100, 150, and 200 kPa. In total 48 tests were performed to compare the different types of stone column conditions, all the cases considered are listed in Table 2.

3. Results of experimental program

3.1 General

The soil bed and soil-stone column combined were tested using the large shear box test apparatus to create the horizontal movement, and graphs of shear stress vs. shear strain were produced. The values of shear stresses for the 25% strain, or 37.5 mm of horizontal displacement, may be seen in Figs. 5-22 to be larger in the case of USC than that of a sand bed. The inclusion of USC in the sand bed improves shear resistance, demonstrating that the stiffness of the combined soil-stone column system is increased when a material with a greater elastic modulus is employed to replace loose soil. Under various circumstances of normal pressure, it was shown that the shear stress in cases of USC was 6–10% greater in cases of single columns and up to 15% higher in cases of groups of stone columns as compared to the sand bed alone. This demonstrates unequivocally that the stronger material present in the shear path has enhanced resistance to the external lateral load at the plane of failure. Shear stress values for the sand bed case at maximum displacement are 76, 106 and 134 kPa under normal pressures of 100, 150 and 200 kPa, respectively. The shear stress values at equal levels of displacement were found to be 81, 112, and 141 kPa in the case of USC. This indicates that a roughly similar amount of shear resistance increases in the USC as well as the sand bed when the normal pressure rises by the same amount. In the present investigation, it is observed that the amount of shear resistance achieved for a sand bed deformed by 25% under lateral load, is reached in the initial 10-15% deformation stage when USC is utilised.

This improves further in confinement situations, where equivalent shear stress resistance is observed between 5 and 10% of deformation. Previous numerical (Jaiswal and Kumar 2022) and experimental (Mohapatra 2016) studies have also found that clear shear of the un-encased stone column body has been observed under lateral load, whereas in the case of encased stone columns, the body showed only a deformed shape at the junction, which can be referred to as the bending of the encased body. As the confined column exhibits the same strength at a lower degree of deformation compared to that of the later-stage sand bed, this change in the soil-stone column combined system could be quite helpful to design the foundation of the structures within the permitted deformation limits.

3.2 Shear modulus/stiffness

The material response of the soil to the shear deformation is represented by the shear modulus. This important feature provides us with an indication of the resistance offered by the material to the shearing-induced deformation. It is measured as the ratio of the shear stress to the shear strain in the material, which is valid for the element A shown in Fig. 4**,** where the shape of the element transformed. The strain can be defined as $\Delta x/X$ whereas shear stress is measured as the ratio of the shear force to the area over which the shear is generated. In the case of a large shear box test setup, as the lower box reaches its final position, the element B presented at the shear plane behaves exactly in the same manner as the element A, due to the shear that occurs at the plane due to the movement of the lower box. Element-B can be considered the equivalent to Element-A; hence, the shear modulus can be used to compare different soil samples or the soil-stone column system as a whole within the large shear box setup.

The initial length of the area is 150 mm, and a 25% (37.5 mm) deformation was generated for the sample for which shear stress-strain graphs have been generated. In the current study, the secant shear modulus for 10% deformation is plotted on shear stress-shear strain graphs for various cases of normal pressure, stone column diameter, and the arrangement. It has been the general observation that the initial tangent modulus of elasticity for all the cases of sand bed, un-encased column and encased column are nearly the same, but as the strain induced in the body increases, the secant modulus at various displacement

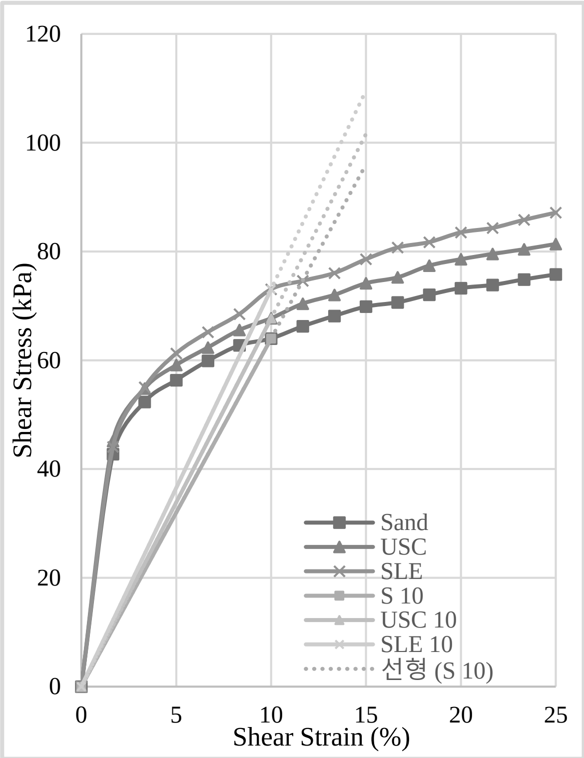

Fig. 5 Shear Stress -Strain curve for 50 mm Diameter single Stone column under 100 kPa Normal Pressure

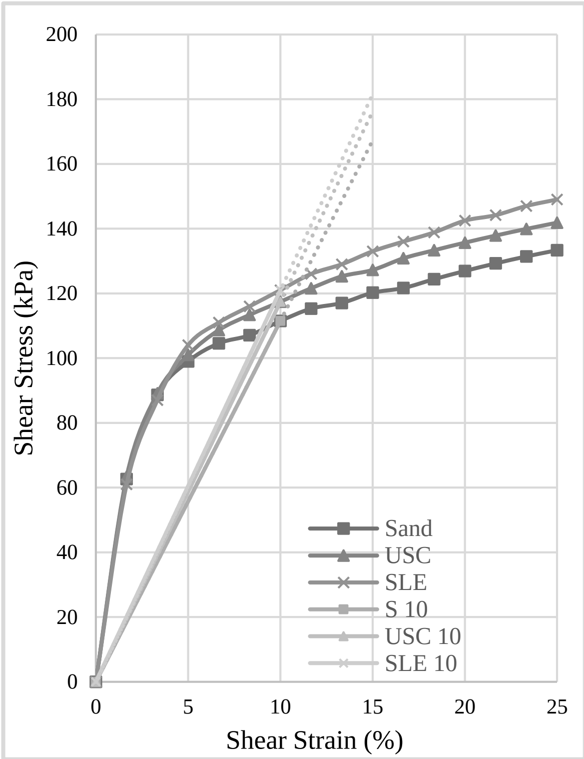

Fig. 7 Shear Stress -Strain curve for 50 mm Diameter single Stone column under 200 kPa Normal Pressure

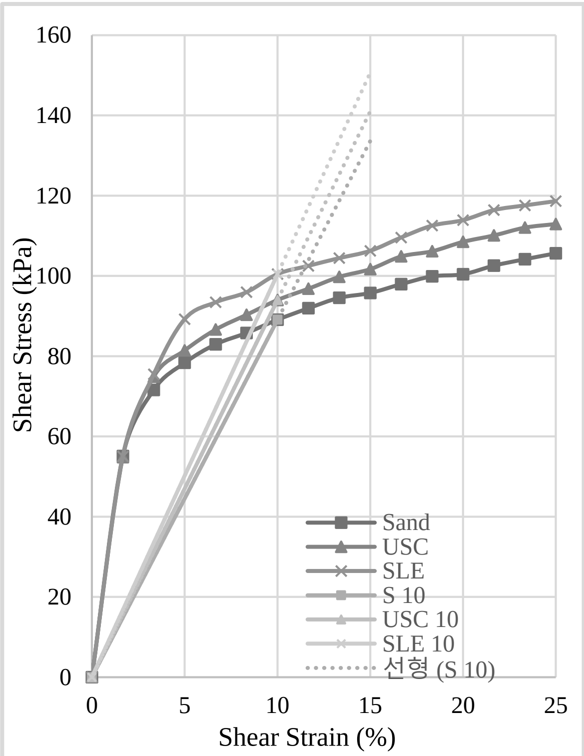

Fig. 6 Shear Stress -Strain curve for 50 mm Diameter single Stone column under 150 kPa Normal Pressure

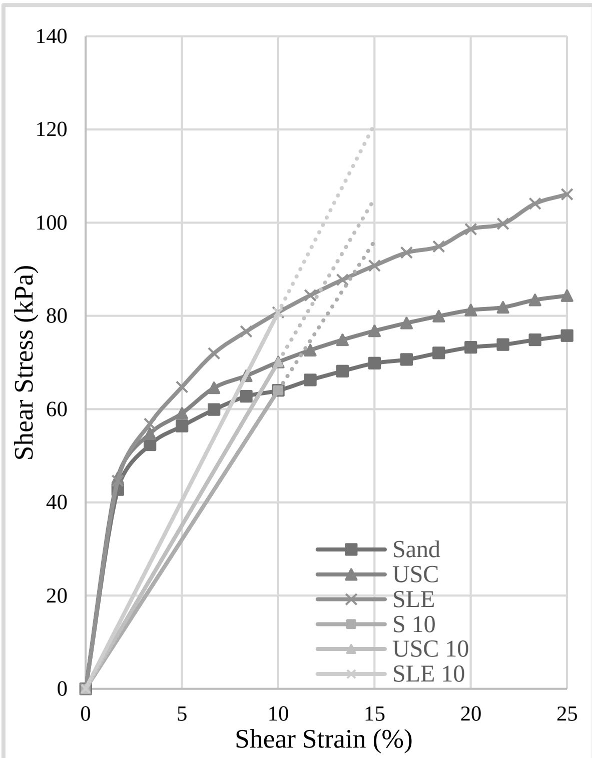

Fig. 8 Shear Stress -Strain curve for 50 mm Diameter, Square Arrangement, 100 kPa Normal Pressure

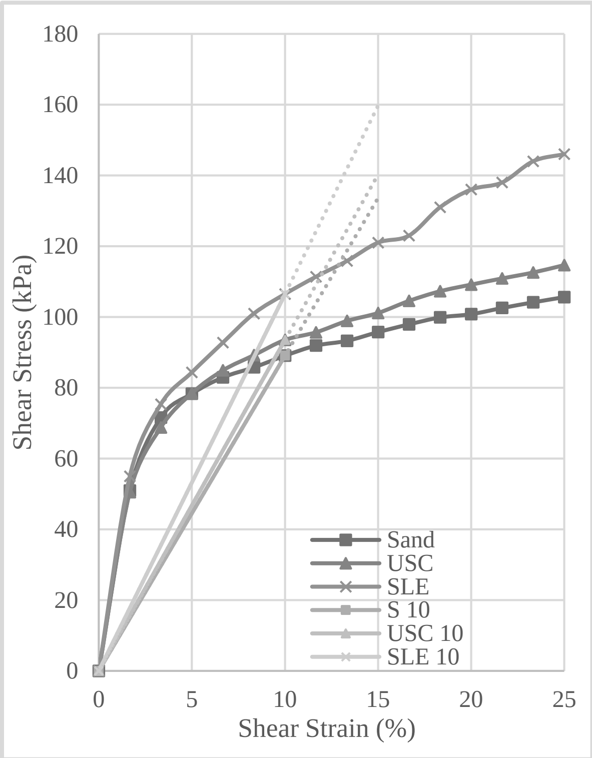

Fig. 9 Shear Stress -Strain curve for 50 mm Diameter, Square Arrangement, 150kPa Normal Pressure

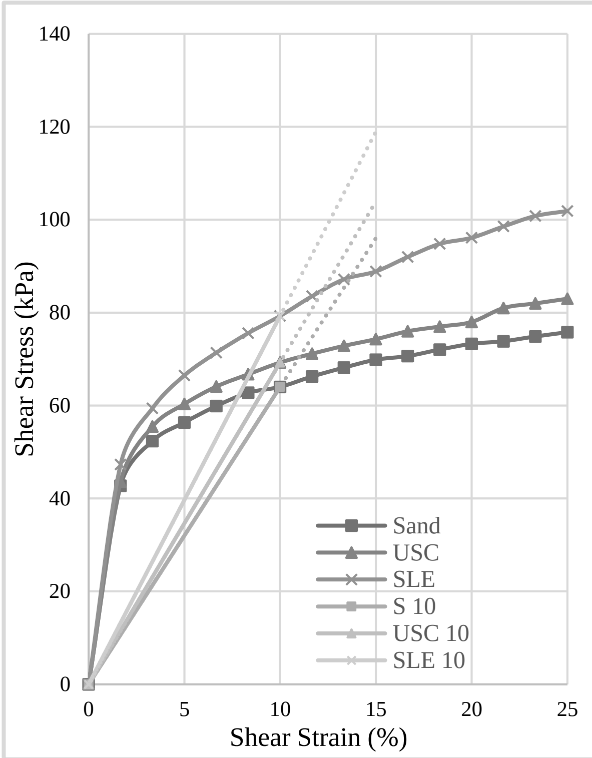

Fig. 11 Shear Stress -Strain curve for 50 mm Diameter, Triangular Arrangement, 100 kPa Normal Pressure

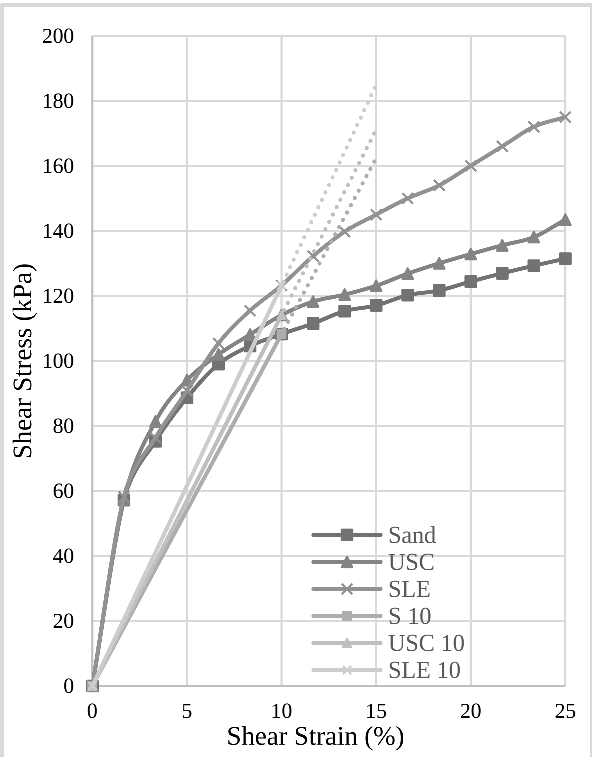

Fig. 10 Shear Stress -Strain curve for 50 mm Diameter, Square Arrangement, 200 kPa Normal Pressure

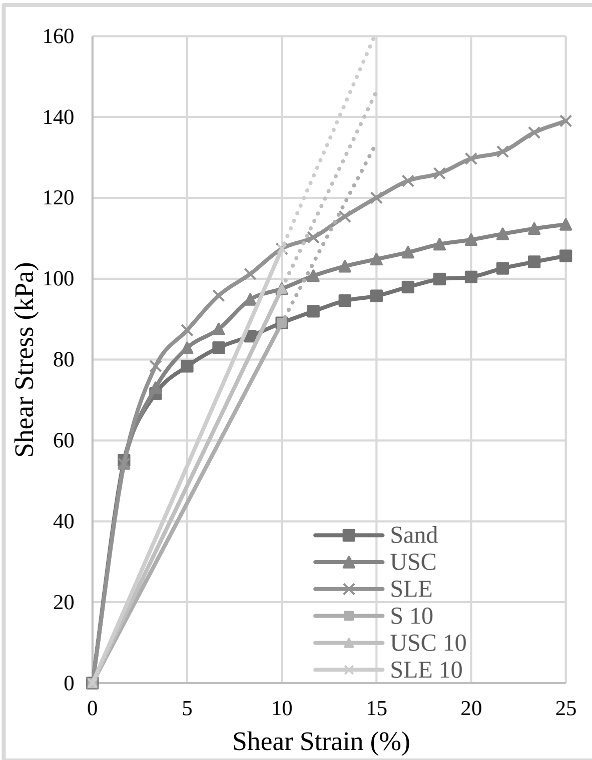

Fig. 12 Shear Stress -Strain curve for 50 mm Diameter, Traingular Arrangement, 150 kPa Normal Pressure

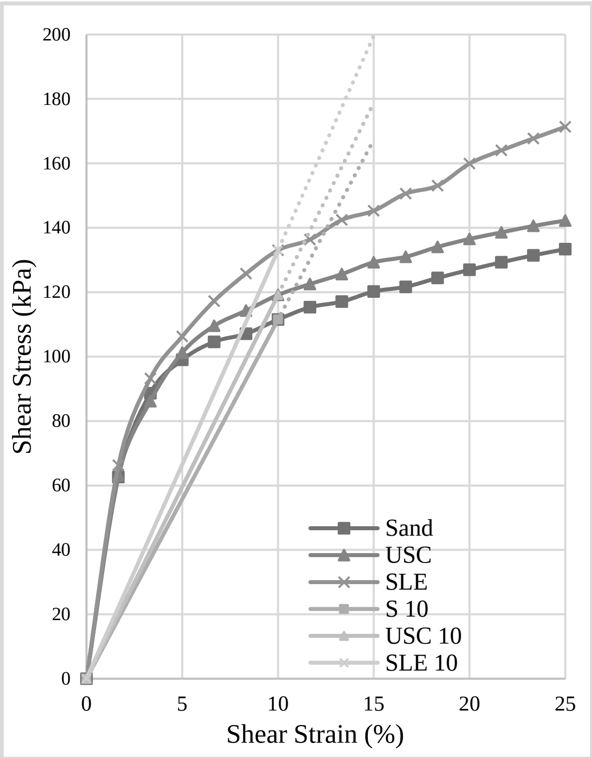

Fig. 13 Shear Stress -Strain curve for 50 mm Diameter, Traingular Arrangement, 200 kPa Normal Pressure

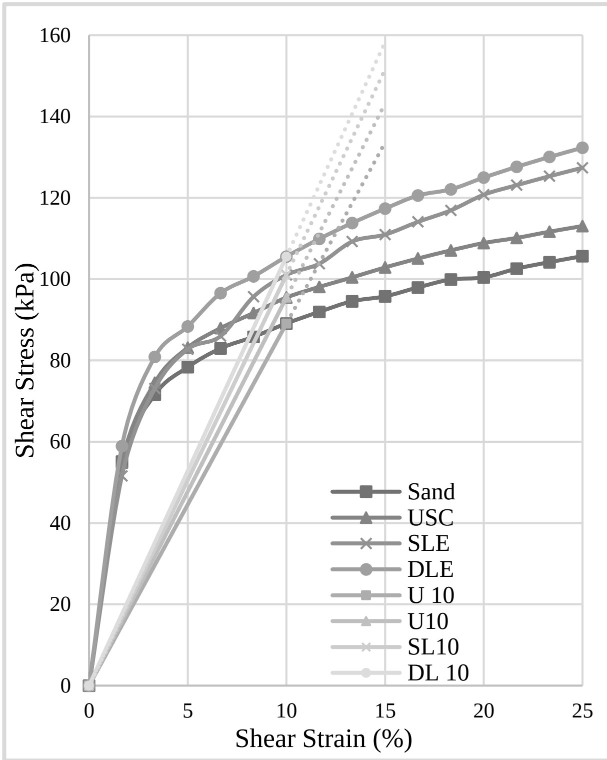

Fig. 15 Shear Stress -Strain curve for 75 mm Diameter, Single Column, 150kPa Normal Pressure

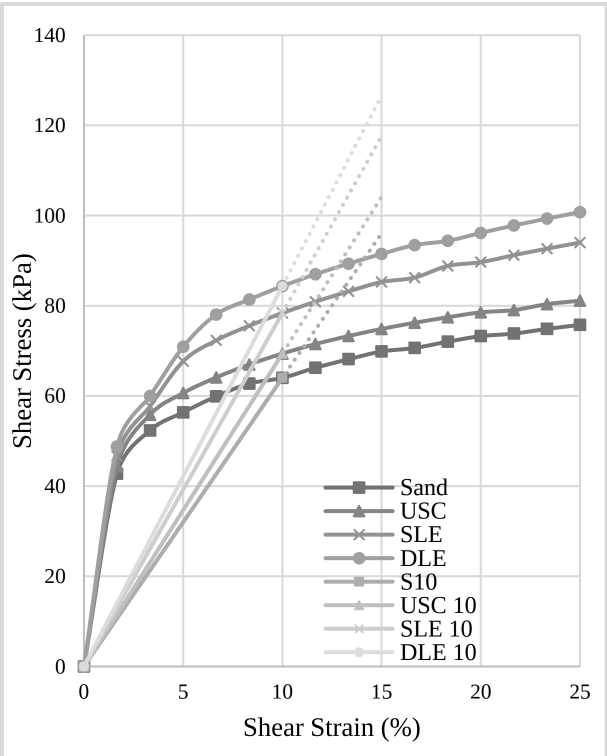

Fig. 14 Shear Stress -Strain curve for 75 mm Diameter, Single Column, 100kPa Normal Pressure

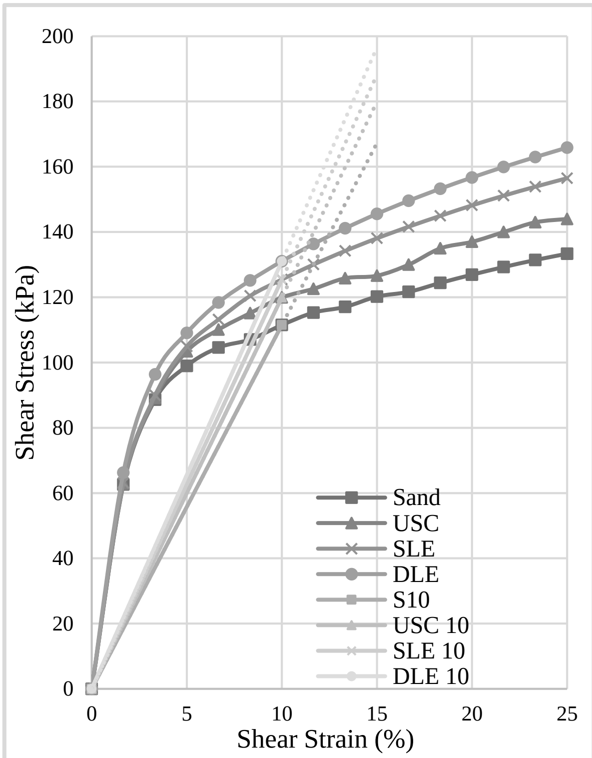

Fig. 16 Shear Stress -Strain curve for 75 mm Diameter, Single Column, 200 kPa Normal Pressure

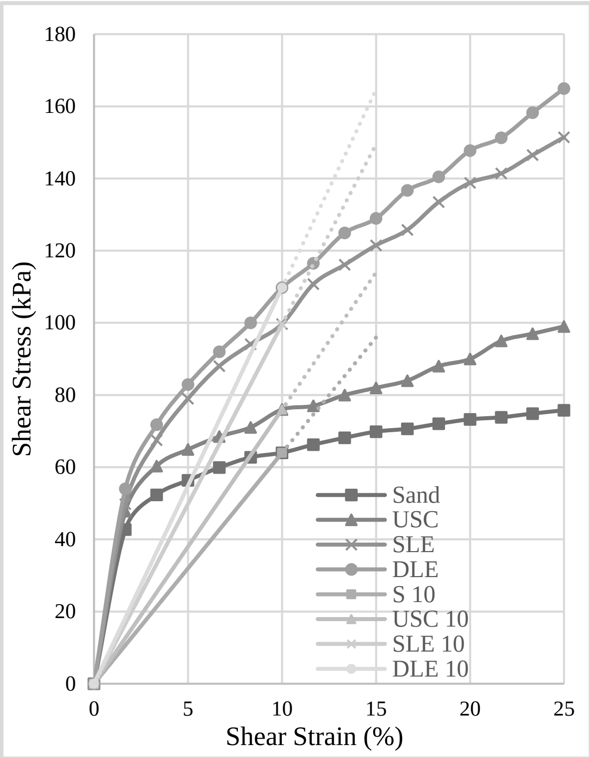

Fig. 17 Shear Stress -Strain curve for 75 mm Dia, Square Arrangement, 100 kPa Normal Pressure

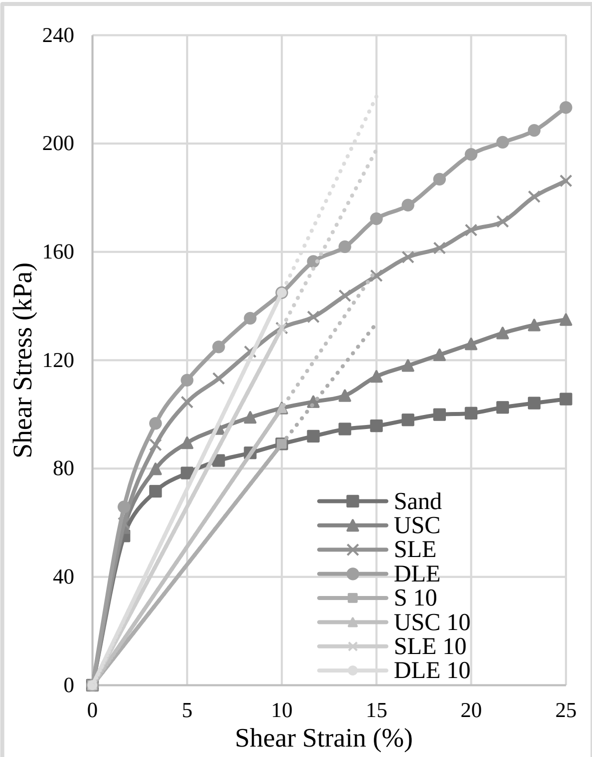

Fig. 18 Shear Stress -Strain curve for 75 mm Dia, Square Arrangement, 150 kPa Normal Pressure

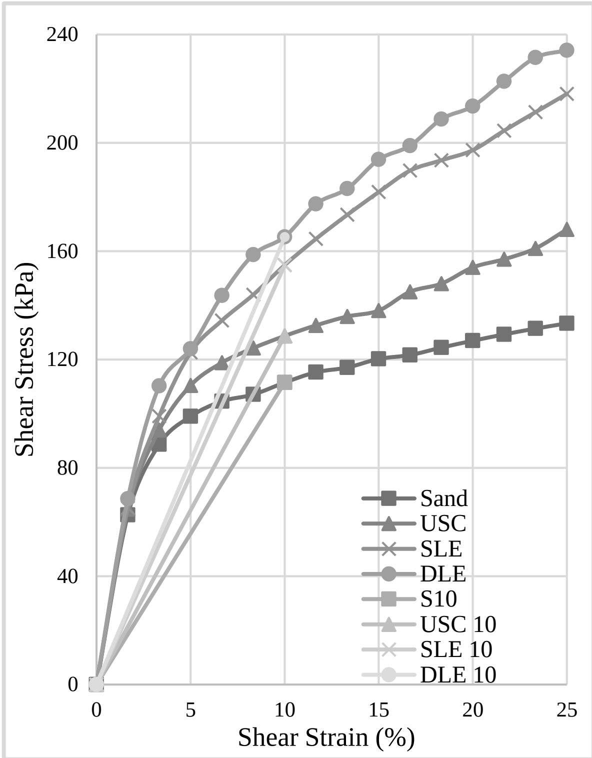

Fig. 19 Shear Stress -Strain curve for 75 mm Dia, Square Arrangement, 200 kPa Normal Pressure

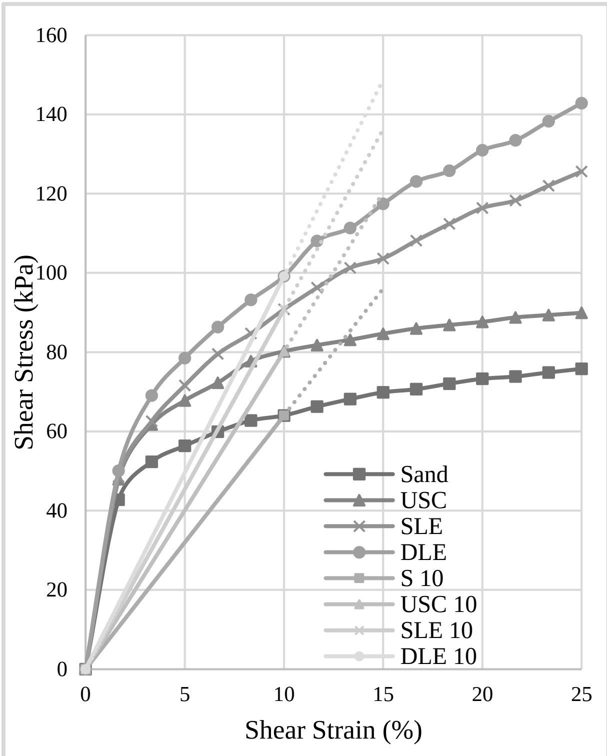

Fig. 20 Shear Stress -Strain curve for 75 mm Dia, Traingular Arrangement, 100 kPa Normal Pressure

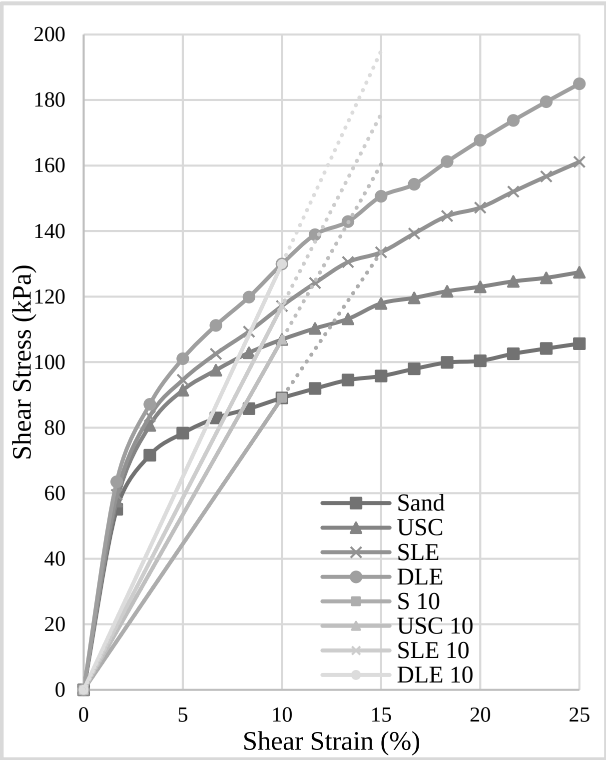

Fig. 21 Shear Stress -Strain curve for 75 mm Diameter, Traingular Arrangement, 150 kPa Normal Pressure

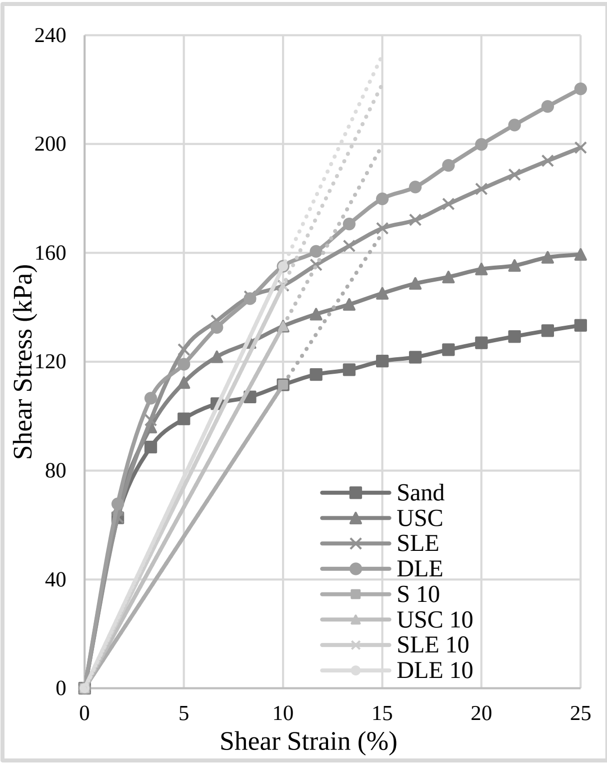

Fig. 22 Shear Stress -Strain curve for 75 mm Diameter, Traingular Arrangement, 200 kPa Normal Pressure

percentages starts to show the variation between the different samples. For a better comparison, the secant modulus of shear has been plotted in all the shear stress-strain curves for the 10% of the deformation through the equation of the slope of the line connecting the origin to the correspondent point of stress indicated by E_{10}. A secant modulus (E_{10}) of 6.4 kN/m^2 was obtained for the case of a sand bed only when tested under the normal pressure of 100 kPa and 6.78, 7.30 kN/m^2 for the case of an un-encased and single-layer encased stone column, respectively, when the single column is installed at the centre. The same is true for other normal pressure conditions (Figs. 5-22). A higher value of E_{10} was observed for combined soil-stone column system when compared to the sand bed only.

The percentage increase in E_{10} from a sand bed to a single-layer encased stone column of 50 mm diameter is 14 % when the test is done for the single column, whereas it increases to 23% and 26% in the grouped stone column test for a triangular and square arrangement, respectively. When the area of replacement is increased and the 75-mm stone column is used, the change in E_{10} for the single column test, the triangular pattern, and the square pattern of a grouped column is 22%, 42%, and 52%, respectively. Which shows that higher shear resistance mobilizes due to the increases in the replacement area because more rigid and compacted material is available at the plane of shear.

3.3 Arrangement of stone column

At normal pressures of 100, 150, and 200 kPa, the shear resistance provided by loose sand is 76,106, and 134 kPa for 25% shear deformation, respectively. This maximum shear resistance shifts to 83,114 and 142 kPa. When a group of 50 mm diameter stone columns is installed in a triangular pattern, and nearly 2-4 kPa higher than the triangular arrangement if a square arrangement is considered, this increment is typically between 6% and 15% higher than the sand bed. When the diameter of the grouped stone column employed is 75 mm, the change in maximum shear stress due to the loose sand bed case increases by 25-30% and 16-18% for square and triangular patterns under various normal pressure circumstances. This increased shear stress mobilisation caused by the stone column group is observed because the predominant area of high strength is available at the plane of shear due to the aggregate or granular material present in the system. Mohapatra *et al*. (2016) further stated that the neighbouring columns generate a confinement effect with each other and the underlying soil, which increases the overall composite body's resilience.

The shear modulus for 10% displacement is plotted against the normal pressure in Figs. 23 and 24 which demonstrates that the shear modulus increases as the normal pressure increases. Due to a higher vertical load or normal pressure, the friction between two surfaces or particles rises, which enhances the shear resistance at the shear plane and the overall rigidity of the body. The fluctuation of the secant shear modulus with normal pressure for various combinations and arrangements of stone columns is depicted in Figs. 23 and 24. The stiffness of the single column sand bed systems is less than that of the grouped

Table 3 Peak shear stress for various cases

Conditions of Sample			Shear stress (kPa) in different encasement conditions		
Diameter of Stone column	Normal Pressure (kPa)	Arrangement	USC	SLE	DLE
50	200	Single	141	149	-
		Triangular	142	171	-
		Square	143	175	-
75		Single	144	156	165
		Triangular	159	198	220
		Square	168	218	234
50	150	Single	112	118	-
		Triangular	114	139	-
		Square	116	146	-
75		Single	113	127	132
		Triangular	127	161	184
		Square	135	186	213
50	100	Single	81	87	-
		Triangular	83	101	-
		Square	86	106	-
75		Single	84	94	100
		Triangular	89	125	142
		Square	99	151	164

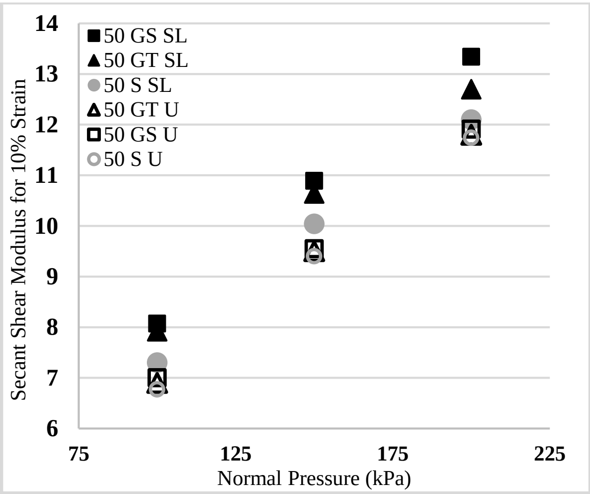

Fig. 23 Variation of Secant Modulus E_{10} for different cases of 50 mm Diameter column

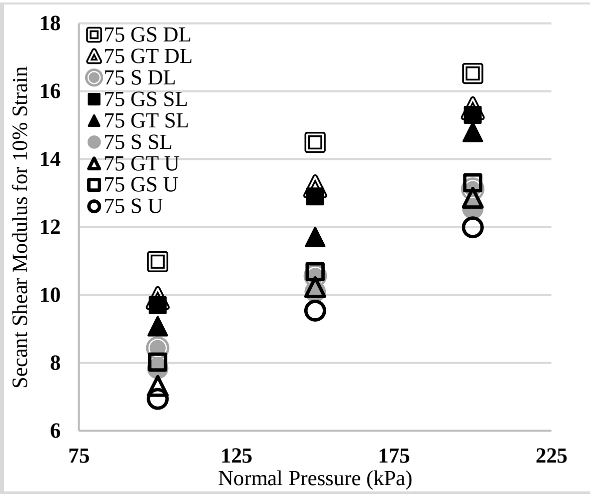

Fig. 24 Variation of Secant Modulus E_{10} for different cases of 75 mm Diameter column

stone column systems. When sand is tested under 100 kPa, the secant shear modulus is 6.4 kN/m^2; this value increases to 6.77, 6.9, and 7.1 kN/m^2 for a single, triangular, and square arrangement, respectively. For un-encased column examples, the biggest shift in system stiffness occurred in the case of a 75 mm stone column with a square pattern, where the secant modulus is 8.02 kN/m^2.

3.4 Effect of encasement conditions

In order to study the effect of the encasement, the encasement is provided for the stone column body. The shear resistance increases at all normal pressure values for encased stone columns, which shows encasing the stone column improves the confinement phenomenon. The slope of the shear stress-strain graphs steepens as the column material is constrained, as shown in Figs. 5-22. It is also noticed that by providing a single-layer of encasement, the change in shear resistance over USC is greater than the change found when USC is provided over a sand bed.

The percentage improvement from USC to SLE is lowest for single column testing, which is 5-12%, this reaches 20-22% for a triangular pattern, and it reaches a maximum of 23-52.5% when a square pattern of arrangement is employed inside the sand sample. The results of the overall composite samples can be seen in Table 3. This shows that the soil between the stone columns acts like stronger soil, so it can be used under structures to give a firm place for the load to be transferred to the surrounding strata.

For the experimental study, 75 mm-diameter stone columns were used to see how the double-layered stone column worked. It has been observed that the DLE stone columns are more effective than the SLE stone columns when subjected to shear. From Figs. 5-22 it is clear that at the later stage of displacements, a significant increase in shear stresses has been observed related to the sand bed. The DLE shows 14-20% enhancement in the shear stresses when compared to an un-encased stone column when a single column has been subjected to lateral displacement under various normal pressures. Similar to the SLE, the addition of shear strength has been observed more in the case of grouped stone columns. For the normal pressure case of 150 kPa, the ratio of shear strength in DLE to an un-encased stone column is 1.45 and 1.58 times for triangular and square patterns of arrangement, respectively.

This improvement is greater in the case of a lower normal pressure of 100 kPa. The shear resistance of DLE is between 1.6 and 1.65 times higher than that of USC.

To test the shear characteristics of the soil-stone column system, the Mohr-Coulomb failure envelopes for a 75 mm group of stone column were produced. Compared to the OGC and SLE stone column installed soil column combined system, the change in angle of internal friction is negligible for DLE cases. However, the value of cohesion for a combined system varies greatly. Cohesion values for a combined system are 30.5 kN/m^2, 84.5 kN/m^2, and 98.6 kN/m^2 for OGC, SLE, and DLE, respectively. Which indicates that the use of DLE stone columns results in 3.2 times greater cohesion in the soil system than the case of unencased stone columns. This improvement in cohesion value is the explanation for the higher resistance offered by the system and is directly visible in the shear strength of a stone column.

Under normal pressure of 100 kPa, the E_{10} obtained for the DLE case in square and triangular patterns is 9.91 kN/m^2 and 10.98 kN/m^2, which are 1.55 and 1.71 times the sand bed, respectively. It is clear how the dual encasing improved the soil-stone column combined system. While the improvement is still considerable when a higher overburden pressure is used, it is 1.48, 1.62, 1.39 and 1.45 times greater in square and triangular patterns when 150 and 200 kPa overburden pressures are used. Square pattern arrangements provide stronger resistance to shear stress, and this resistance rises to its highest level in dual-layered encasements. The field where embankments require the stronger base of stone columns and where the edge lines of stone columns are susceptible to shear force due to the soil's propensity to form a slip circle can be considered an application for the improvement in shear resistance.

4. Conclusions

The effects of conventional stone columns on soil shear strength, as well as the effects of different stone column encasement conditions, were experimentally investigated. The soil bed and soil-stone column combined body were tested using a large shear box to simulate 25% horizontal movement. When loose sand is replaced with a soil-stone column combination system, that often performs better under shear deformation. Some of the main findings are: -

- Observations indicate that the amount of shear resistance achieved for a deformed sand bed under lateral load is identical to the degree of resistance attained at the initial deformation stage when USC or confinement is being used. Un-encased stone column sections shear under lateral force, whereas encased bodies just bend at the shear plane.
- Within the sand sample, the percentage change in shear resistance from USC to SLE ranges from 5 to 53%, with single column shear resistance improvements being the lowest and square arrangement improvements being the highest.
- The ratio of shear strength in DLE to an un-encased stone column for considering normal pressures in the study is 1.4 to 1.7 for triangular and square patterns of arrangement. Lower normal pressures resulted in greater improvement and better shear resistance for DLE when compared to USC.
- The stiffness of the system depends on the area of the bed that stone columns replace. A greater diameter stone column inserted into the system shows a higher secant modulus at the 10% shear strain.
- A dual-layer enclosed column exhibits a greater E_{10} value than a loose sand bed, with the highest level of improvement of up to 1.7 times in the case of a square arrangement.

Acknowledgments

No funding or financial assistance was provided for the research and/or preparation of the manuscript.

References

Abusharar, S.W. and Han, J. (2011), "Two-dimensional deep-seated slope stability analysis of embankments over stone column improved soft clay", *Eng. Geol.*, **120**, 103-110. https://doi.org/10.1016/j.enggeo.2011.04.002.

Abhishek, S.V., Rajyalakshmi, K. and Madhav, M.R. (2016), "Engineering of ground with granular piles: a critical review", *Int. J. Geotech. Eng.*, **10**(4), 337-357. https://doi.org/10.1080/19386362.2016.1145942.

Aghili, E., Hosseinpour, I., Chenari, R.J. and Ahmadi, H. (2021), "Behavior of granular column-improved clay under cyclic shear loading", *Transport. Geotech.*, **31**, 100654. https://doi.org/10.1016/j.trgeo.2021.100654.

Alexiew, D., Brokemper, D. and Lothspeich, S. (2005), "Geotextile encased columns (GEC): load capacity, geotextile selection and pre-design Graphs", *Proceedings of the Contemporary issues in Foundation Engineering, Geo-Frontiers Congress,* Austin, Texas, January. https://doi.org/10.1061/40777(156)12.

Ali, K., Shahu, J.T. and Sharma, K.G. (2014), "Model tests on single and groups of stone columns with different geosynthetic reinforcement arrangement", *Geosynth. Int.*, **21**(2), 103-118. https://doi.org/10.1680/gein.14.00002.

Alkhorshid, N.R., Araujo, G.L., Palmeira, E.M. and Zornberg, J. G. (2019), "Large-scale load capacity tests on a geosynthetic encased column", *Geotext. Geomembranes*, **47**(5), 632-641. https://doi.org/10.1016/j.geotexmem.2019.103458.

Almeida, M.S., Hosseinpour, I., Riccio, M. and Alexiew, D. (2015), "Behavior of geotextile-encased granular columns supporting test embankment on soft deposit", *J. Geotech. Geoenviron. Eng.*, **141**(3), 04014116. https://doi.org/10.1061/(ASCE)GT.1943-5606.0001256.

Almeida, M.S.S., Hosseinpour, I. and Riccio, M. (2013), "Performance of a geosynthetic-encased column (GEC) in soft ground: numerical and analytical studies", *Geosynthetics Int.*, **20**(4), 252-262. https://doi.org/10.1680/gein.13.00015.

Bhattacharya, P. and Kumar, J. (2017), "Bearing capacity of foundations on soft clays with granular column and trench", *Soils Found.*, **57**(3), 488-495. https://doi.org/10.1016/j.sandf.2017.05.013.

Brokemper, D., Sobolewski, J., Alexiew, D. and Brok, C. (2006), "Design and construction of geotextile encased columns supporting geogrid reinforced landscape embankments", *Proceeding of the 8th International Conference on Geosynthetics*, Bastions Vijfwal Houten in the Netherlands,October.

Basack, S., Indraratna, B., Rujikiatkamjorn, C. and Siahaan, F. (2017), "Modeling the stone column behavior in soft ground with special emphasis on lateral deformation", *J. Geotech. Geoenviron. Eng.*, **143**(6), 04017016. https://doi.org/10.1061/(ASCE)GT.1943-5606.0001652.

Black, J.A., Sivakumar, V., Madhav, M.R. and Hamill, G.A. (2007), "Reinforced stone columns in weak deposits: laboratory model study", *J. Geotech. Geoenviron. Eng.*, **133**(9), 1154-1161. https://doi.org/10.1061/(ASCE)1090-0241(2007)133:9(1154).

Castro, J., Cimentada, A., da Costa, A., Cañizal, J. and Sagaseta, C. (2013), "Consolidation and deformation around stone columns: Comparison of theoretical and laboratory results", *Comput. Geotech.*, **49**, 326-337. https://doi.org/10.1016/j.compgeo.2012.09.004.

Cengiz, C., Kilic, I. E. and Guler, E. (2019), "On the shear failure mode of granular column embedded unit cells subjected to static and cyclic shear loads", *Geotext. Geomembranes*, **47**(2),193-202. https://doi.org/10.1016/j.geotexmem.2018.12.011.

Chen, J.F., Li, L.Y., Xue, J.F. and Feng, S.Z. (2015), "Failure mechanism of geosynthetic-encased stone columns in soft soils under embankment", *Geotext. Geomembranes*, **43**(5), 424-431. https://doi.org/10.1016/j.geotexmem.2015.04.016.

Chen, R.P., Chen, Y.M., Han, J. and Xu, Z.Z. (2008), "A theoretical solution for pile-supported embankments on soft soils under one-dimensional compression", *Can. Geotech. J.*, **45**(5), 611-623. https://doi.org/10.1139/T08-003.

Castro, J. and Sagaseta, C. (2011), "Deformation and consolidation around encased stone columns", *Geotext. Geomembranes*, **29**(3), 268-276. https://doi.org/10.1016/j.geotexmem.2010.12.001.

Das, A.K. and Deb, K. (2017), "Modeling of stone column-supported embankment under axi-symmetric condition", *Geotech. Geol. Eng.*, **35**(2), 707-730. https://doi.org/10.1007/s10706-016-0136-1.

Dash, S.K. and Bora, M.C. (2013), "Influence of geosynthetic encasement on the performance of stone columns floating in soft clay", *Can. Geotech. J.*, **50**(7), 754-765. https://doi.org /10.1139/cgj-2012-0437.

Dash, S.K., Rajagopal, K. and Krishnaswamy, N.R. (2004), " Performance of different geosynthetic reinforcement materials in sand foundations", *Geosynthetics Int*., **11**(1), 35-42. https://doi.org /10.1680/gein.2004.11.1.35.

Deb, K. and Mohapatra, S.R. (2013), "Analysis of stone column-supported geosynthetic-reinforced embankments", *Appl. Math. Model.*, **37**(5), 2943-2960. https://doi.org/10.1016/j.apm.2012.07.002.

Deb, K. and Dhar, A. (2011), "Optimum design of stone column-improved soft soil using multiobjective optimization technique", *Comput. Geotech.*, **38**(1), 50-57 https://doi.org/10.1016/j.compgeo.2010.10.005.

Elsawy, M.B.D. (2013), "Behaviour of soft ground improved by conventional and geogrid-encased stone columns, based on FEM study", *Geosynthetics Int*., **20**(4), 276-285. https://doi.org/10.1680/gein.13.00017.

Fox, Z.P. (2011), "Critical state, dilatancy and particle breakage of mine waste rock", Master's Thesis, Colorado State University, Fort Collins, USA.

Guo, X., Zhang, H. and Liu, L. (2020), "Planar geosynthetic-reinforced soil foundations: a review", *SN Appl. Sci.*, **2**, 1-18. https://doi.org/10.1007/s42452-020-03930-5.

Gao, J., Zhang, Y., Wang, C. and Yuan, C. (2021), "Behavior characteristics of geosynthetic-encased stone column under cyclic loading", *Transport. Geotech.*, **28**, 100554. https://doi.org/10.1016/j.trgeo.2021.100554.

Gniel, J. and Bouazza, A. (2009), "Improvement of soft soils using geogrid encased stone columns", *Geotext. Geomembranes*, **27**(3), 167-175. https://doi.org/10.1016/j.geotexmem.2008.11.001.

Gniel, J. and Bouazza, A. (2010), "Construction of geogrid encased stone columns: A new proposal based on laboratory testing", *Geotext. Geomembranes*, **28**(1), 108-118. https://doi.org/10.1016/j.geotexmem.2009.12.012.

Gholaminejad, A., Mahboubi, A. and Noorzad, A. (2020), "Encased stone columns: coupled continuum–discrete modelling and observations", *Geosynthetics Int.*, **27**(6), 581-592.

Ghazavi, M. and Afshar, J.N. (2013), "Bearing capacity of geosynthetic encased stone columns", *Geotext. Geomembranes*, **38**, 26-36. https://doi.org/10.1016/j.geotexmem.2013.04.003.

Gu, M., Han, J. and Zhao, M. (2020), "Three-dimensional DEM analysis of axially loaded geogrid-encased stone column in clay bed", *Int. J. Geomech.*, **20**(3), 04019180. https://doi.org/10.1061/(ASCE)GM.1943-5622.0001595.

Hosseinpour, I., Almeida, M.S.S. and Riccio, M. (2016), "Ground improvement of soft soil by geotextile-encased columns", *Proc. Inst. Civil Engineers-Ground Improvement*, **169**(4), 297-305, https://doi.org/10.1680/jgrim.16.00009.

Han, J. and Gabr, M.A. (2002), "Numerical *analysis* of geosynthetic reinforced and pile-supported earth platforms over soft soil", *J. Geotech. Geoenviron. Eng.*, **128**(1), 44-53. https://doi.org/10.1061/(ASCE)1090-0241(2002)128:1(44).

Han, J. and Ye, S.L., (2001), "Simplified method for consolidation rate of stone column reinforced foundations"; *J. Geotech. Geoenviron. Eng. ASCE*, **127**(7), 597-603. https://doi.org/10.1061/(ASCE)1090-0241(2001)127:7(597).

Han, J., Huang, J. and Porbaha, A. (2005), "2D numerical modeling of a constructed geosynthetic-reinforced embankment over deep mixed columns", *In: ASCE Geotechnical Special Publication (GSP) No.131, Contemporary Issues in Foundation Engineering, ASCE GeoFrontiers, 1-11*, Austin (TX), January. https://doi.org/10.1061/40777(156)13.

Hewlett, W.J. (1988), "Analysis of piled embankment", *Ground Engrg.*, **21**(3), 12-18

Indraratna, B., Basack, S. and Rujikiatkamjorn, C. (2013), "Numerical solution of stone column improved soft soil considering arching, clogging and smear effects", *J. Geotech. Geoenviron. Eng.*, **139**(3), 377-394**.** https://doi.org/10.1061/(ASCE)GT.19435606.0000789.

Jaiswal, A. and Kumar, R. (2022), "Finite element analysis of granular column for various encasement conditions subjected to shear load", *Geomech. Eng.*, **29**(6), 645-655. https://doi.org/10.12989/gae.2022.29.6.645.

Khabbazian, M., Kaliakin, V.N. and Meehan, C.L. (2015), "Column supported embankments with geosynthetic encased columns: validity of the unit cell concept", *Geotech. Geol. Eng.*, **33**, 425-442. https://doi.org/10.1007/s10706-014-9826-8.

Khajeh, A., Ebrahimi, S.A., Mola Abasi, H., Jamshidi Chenari, R. and Payan, M. (2021), "Effect of EPS beads in lightening a typical zeolite and cement-treated sand", *Bull. Eng. Geol. Environ.*, **80**(11), 8615-8632. https://doi.org/10.1007/s10064-021-02458-1.

Khajeh, A., Jamshidi Chenari, R. and Payan, M. (2020), "A simple review of cemented non-conventional materials: soil composites", *Geotech. Geol. Eng.*, **38**, 1019-1040. https://doi.org/10.1007/s10706-019-01090-x.

Khajeh, A., Jamshidi Chenari, R. and Payan, M. (2020), "A review of the studies on soil-EPS composites: beads and blocks", *Geotech. Geol. Eng.*, **38**, 3363-3383. https://doi.org/10.1007/s10706-020-01252-2.

Khajeh, A., Jamshidi Chenari, R., Mola Abasi, H. and Payan, M. (2022), "An experimental investigation on geotechnical properties of a clayey soil stabilised with lime and zeolite in base and subbase courses", *Road Mater. Pavement Design*, **23**(12), 2924-2941. https://doi.org/10.1080/14680629.2021.1997789.

Khaksar Najafi, E., Jamshidi Chenari, R., Payan, M. and Arabani, M. (2021), "A sustainable landfill liner material: clay-fly ash geopolymers", *Bull. Eng. Geol. Environ.*, **80**, 4111-4124. https://doi.org/10.1007/s10064-021-02185-7.

Khaksar Najafi, E., Jamshidi Chenari, R., Payan, M. and Arabani, M. (2021), "Compositional effects of clay–fly ash geopolymers on the sorption process of lead and zinc", *J. Environ. Quality*, **50**(3), 768-781. https://doi.org/10.1002/jeq2.20207.

Katti, R.K., Katti, A.R. and Naik, S. (1993), "Monograph to analysis of stone columns with and without geosynthetic encasement", CBIP Publication, New Delhi, India.

Kowalski, T.E., Starry, D.W. and America, J.W. (2007), "Modern soil stabilization techniques", *Proceedings of the Annual Conference of the Transportation Association of Canada*, Saskatoon, Saskatchewan, October.

Kong, G., Zhou, Y. and Liu, H. (2018), "Nonlinear model analysis of radial bulging deformation of geosynthetic-encased stone columns", *Int. J. Geomech.*, **18**(10), 06018022. https://doi.org/10.1061/(ASCE)GM.1943-5622.0001195.

Kitazume, M. and Maruyama, K. (2007), "Internal stability of group column type deep mixing improved ground under embankment loading", *Soils Found.*, **47**(3), 437-455. https://doi.org/10.3208/sandf.47.437.

Kitazume, M. and Maruyama, K. (2006), "External stability of group column type deep mixing improved ground under embankment loading", *Soils Found.*, **46**(3), 323-340. https://doi.org/10.3208/sandf.46.323.

Low, B.K., Tang, S.K. and Choa, V. (1994), "Arching in piled embankments", *J. Geotech. Eng.*, **120**(11), 1917-1938. https://doi.org/10.1061/(ASCE)0733-410(1994)120:11(1917).

Li, L.Y., Rajesh, S. and Chen, J.F. (2021), "Centrifuge model tests on the deformation behavior of geosynthetic-encased stone column supported embankment under undrained condition", *Geotext. Geomembranes*, **49**(3), 550-563. https://doi.org/10.1016/j.geotexmem.2020.11.003.

Lima, B.T., Almeida, M.S. and Hosseinpour, I. (2022), "Field measured and simulated performance of a stone columns-strengthened soft clay deposit", *Int. J. Geotech. Eng.*, **16**(6), 776-785. https://doi.org/10.1080/19386362.2019.1653506.

Malarvizhi, S.N. and Ilamparuthi, K. (2007), "Comparative study on the behavior of encased stone column and conventional stone column", *Soils Found.*, **47**(5), 873-885. https://doi.org/10.3208/sandf.47.873.

Martin, L., Alizadeh, V. and Meegoda, J. (2019), "Electro-osmosis treatment techniques and their effect on dewatering of soils, sediments, and sludge: A review", *Soils Found.*, **59**(2), 407-418. https://doi.org/10.1016/j.sandf.2018.12.015.

Murugesan, S. and Rajagopal, K. (2006), "Geosynthetic-encased stone columns: numerical evaluation", *Geotext. Geomembranes*, **24**(6), 349-358. https://doi.org/10.1016/j.geotexmem.2006.05.001.

Murugesan, S. and Rajagopal, K. (2007), "Model tests on geosynthetic-encased stone columns", *Geosynthetics Int.*, **14**(6), 346-354. https://doi.org/10.1680/gein.2007.14.6.346.

Maheshwari, P. and Chauhan, V.B. (2013), "Beams on extensible geosynthetics and stone-column-improved soil", *Proceedings of the Institution of Civil Engineers-Ground Improvement*, India, November. https://doi.org/10.1680/grim.12.00005.

McCabe, B., Kamrat-Pietraszewska, D. and Egan, D. (2013)," Ground heave induced by installing stone columns in clay soils", *Proceedings of the Institution of Civil Engineers - Geotechnical Engineering*, India, December. https://doi.org/10.1680/geng.12.00103.

McKenna, J.M., Eyre, W.A. and Wolstenholme, D.R. (1975), "Performance of an embankment supported by stone columns in soft ground", *Geotechnique*, **25**(1), 51-59. https://doi.org/10.1680/geot.1975.25.1.51.

Mitchell, J.K. and Huber, T.R. (1985), "Performance of a stone column foundation", *J. Geotech. Eng.*, **111**(2), 205-223. https://doi.org/10.1061/(ASCE)0733-9410(1985)111:2(205).

Murugesan, S. and Rajagopal, K. (2010), "Studies on the behavior of single and group of geosynthetic encased stone columns", *J. Geotech. Geoenviron. Eng*., **136**, 129-139. https://doi.org/10.1061/(ASCE)GT.1943-5606.0000187.

Mohapatra, S.R., Rajagopal, K. and Sharma, J. (2016), "Direct shear tests on geosynthetic-encased granular columns", *Geotext. Geomembranes*, **44**, 396-405. https://doi.org/ 10.1016/j.geotexmem.2016.01.002.

Murty, V.R. and Praveen, G.V. (2008), "Use of chemically stabilized soil as cushion material below light weight structures founded on expansive soils*", J. Mater. Civil Eng.*, **20**(5), 392-400. https://doi.org/10.1061/(ASCE)0899-1561(2008)20:5(392).

Naeini, S.A. and Gholampoor, N. (2019), "Effect of geotextile encasement on the shear strength behavior of stone column-treated wet clays", *Indian Geotech. J.*, **49**(3), 2 92-303. https://doi.org/10.1007/s40098-018-0329-z.

Nazariafshar J. and Aslani, M. (2020), "Effect of stress concentration ratio on shear strength of soft soils improved with stone columns", *Iran J. Sci. Technol. T. Civil Eng.*, **45**(1-4), 1-20. http://doi.org/10.1007/s40996-020-00391-z..

Ng, K.S. and Tan, S.A. (2015), "Stress transfer mechanism in 2D and 3D unit cell models for stone column improved ground", *Int. J. Geosynth. Ground Eng.*, **1**(3). https://doi.org/10.1007/s40891-014-0003-1.

Nayak, N.V. (1983), "Recent advances in ground improvements by stone column", *Proceedings of the Indian Geotechnical Conference, Madras*.

Ou Yang, F., Zhang, J.J., Liao, W.M., Han, J.W., Tang, Y.L. and Bi, J.B. (2017), "Characteristics of the stress and deformation of geosynthetic-encased stone column composite ground based on large-scale model tests", *Geosynthetics Int*., **24**(3), 242-254. https://doi.org/10.1680/jgein.16.00028

Phani Kumar, B.R. and Sharma, R.S. (2004), "Effect of fly ash on engineering properties of expansive soils", *J. Geotech. Geoenviron. Eng.*, **130**(7), 764-767. https://doi.org/10.1061/(ASCE)1090-0241(2004)130:7(764).

Poorooshasb, H.B., and Meyerhof, G.G. (1996), "Consolidation settlement of rafts supported by stone columns", *Geotech. Eng.*, **27**, 83-92.

Priebe, H.J. (1995), "The design of vibro replacement", *Ground Eng.*, **28**(10), 31.

Pulko, B., Majes, B. and Logar, J. (2011), "Geosynthetic-encased

stone columns: analytical calculation model", *Geotext. Geomembranes*, **29**(1), 29-39. https://doi.org/10.1016/j.geotexmem.2010.06.005.
Raithel, M., Kirchner, A., Schade, C. and Leusink, E. (2005), "Foundation of constructions on very soft soils with geotextile encased columns-state of the art", *Geotech. Special Publication*, **136**. https://doi.org/10.1061/40783(162)20.
Raithel, M. and Kempfert, H.G. (2000), "Calculation models for dam foundations with geotextile-coated sand columns", *Proceedings of the ISRM International Symposium*, Melbourne, Australia, November.
Sadr, A. and Hataf, N. (2021), "Experimental and analytical study on soil bag and encased sand columns in loose sand", *Transport. Geotech.*, **29**, 100553. https://doi.org/10.1016/j.trgeo.2021.100553.
Shahu, J.T. and Reddy, Y.R. (2014), "Estimating long-term settlement of floating stone column groups", *Can. Geotech. J.*, **51**(7), 770-781. https://doi.org/10.1139/cgj-2012-0477.
Shirmohammadi, S., Ghaffarpour Jahromi, S., Payan, M. and Senetakis, K. (2021), "Effect of lime stabilization and partial clinoptilolite zeolite replacement on the behavior of a silt-sized low-plasticity soil subjected to freezing–thawing cycles", *Coatings*, **11**(8), 994. https://doi.org/10.3390/coatings11080994.
Stoeber, J.N. (2012), "Effects of maximum particle size and samplescaling on the mechanical behavior of mine waste rock;Article state approach", Master's Thesis, Colorado State University, Fort Collins, USA.
Terzaghi, K. (1944), "*Theoretical Soil Mechanics*", Chapman and Hali, Limited John Wiler and Sons. Inc, New York USA.
Van Impe, W.F. (1989), "*Soil improvement techniques and their evolution"*, Balkema, Rotterdam, Netherlands.
Wu, C.S. and Hong, Y.S. (2014), "A simplified approach for evaluating the bearing performance of encased granular columns", *Geotext. Geomembranes*, **42**(4), 339-347. https://doi.org/10.1016/j.geotexmem.2014.05.006.
Xu, Z., Zhang, L. and Zhou, S. (2021), "Influence of encasement length and geosynthetic stiffness on the performance of stone column: 3D DEM-FDM coupled numerical investigation", *Comput. Geotech.*, **132**, 103993. https://doi.org/10.1016/j.compgeo.2020.103993.
Xue, J., Liu, Z. and Chen, J. (2019), "Triaxial compressive behaviour of geotextile encased stone columns", *Comput. Geotech.*, **108**, 53-60. https://doi.org/10.1016/j.compgeo.2018.12.010.
Yoo, C. (2010), "Performance of geosynthetic-encased stone columns in embankment construction: numerical investigation", *J. Geotech. Geoenviron. Eng.*, **136**(8), 1148-1160. https://doi.org/10.1061/(ASCE)GT.1943-5606.0000316.
Yoo, C. and Lee, D. (2012), "Performance of geogrid-encased stone columns in soft ground: full-scale load tests", *Geosynthetics Int.*, **19**(6), 480-490. https://doi.org/10.1680/gein.12.00033.
Yun-Min, C., Wei-Ping, C. and Ren-Peng, C. (2008), "An experimental investigation of soil arching within basal reinforced and unreinforced piled embankments", *Geotext. Geomembranes*, **26**(2), 164-174. https://doi.org/10.1016/j.geotexmem.2007.05.004.
Zhou, Y. and Kong, G. (2019), "Deformation analysis of a geosynthetic-encased stone column and surrounding soil using cavity-expansion model", *Int. J. Geomechanics*, **19**(5), 04019036. https://doi.org/10.1061/(ASCE)GM.1943-5622.0001418.
Zhou, Y. and Kong, G. (2019), "Deformation analysis of geosynthetic-encased stone column–supported embankment considering radial bulging", *Int. J. Geomechanics*, **19**(6), 04019057. https://doi.org/10.1061/(ASCE)GM.1943-5622.0001426.
Zhang, Y., Chan, D. and Wang, Y. (2012), "Consolidation of composite foundation improved by geosynthetic-encased stone columns", *Geotext. Geomembranes*, **32**, 10-17. https://doi.org/10.1016/j.geotexmem.2011.10.006.

CC